

# Duoduo CLIP: Efficient 3D Understanding with Multi-View Images

Han-Hung Lee<sup>1,\*</sup> Yiming Zhang<sup>1,\*</sup> Angel X. Chang<sup>1,2</sup>

<sup>1</sup>Simon Fraser University, <sup>2</sup>Canada CIFAR AI Chair, Amii  
{h1a300, yza440, angelx}@sfu.ca  
<https://github.com/3dlg-hcvc/DuoduoCLIP>

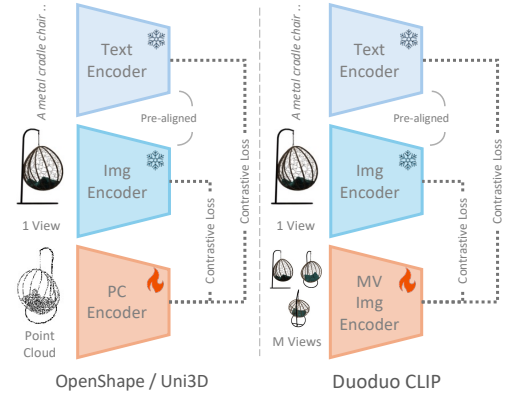
## Abstract

We introduce Duoduo CLIP, a model for 3D representation learning that learns shape encodings from multi-view images instead of point-clouds. The choice of multi-view images allows us to leverage 2D priors from off-the-shelf CLIP models to facilitate fine-tuning with 3D data. Our approach not only shows better generalization compared to existing point cloud methods, but also reduces GPU requirements and training time. In addition, we modify the model with cross-view attention to leverage information across multiple frames of the object which further boosts performance. Compared to the current SOTA point cloud method that requires 480 A100 hours to train 1 billion model parameters we only require 57 A5000 hours and 87 million parameters. Multi-view images also provide more flexibility in use cases compared to point clouds. This includes being able to encode objects with a variable number of images, with better performance when more views are used. This is in contrast to point cloud based methods, where an entire scan or model of an object is required. We showcase this flexibility with object retrieval from images of real-world objects. Our model also achieves better performance in more fine-grained text to shape retrieval, demonstrating better text-and-shape alignment than point cloud based models.

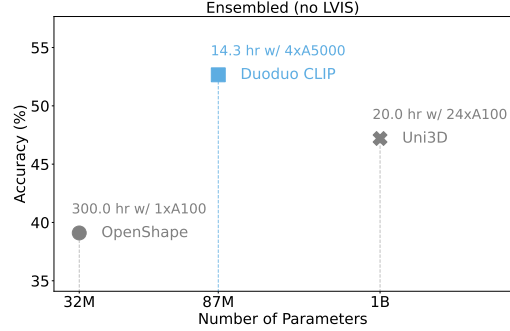
## 1 Introduction

Learning representations for 3D shapes is increasingly useful with growing applications in object generation, shape understanding, grounding and robotics. In recent years, there has also been growing interest in 3D representations that are semantically aligned with text. By having a 3D representation aligned to language, these representations can easily be used for text-to-3D shape retrieval [36, 41, 45] and generation [4], or as a basis for 3D feature maps that can be queried with text [16, 19, 25].

Initial work in this domain [4, 36, 41] attempted to train such aligned models on limited data. More recent work [25, 49] leveraged large pre-trained vision-language models (e.g. CLIP [35]) that already align the text and image embeddings. ULIP [49] used frozen CLIP text-image encoders, and trained only the point-cloud encoder but was still limited due to the limited number of 3D objects as well as paired text captions. With larger 3D datasets like Objaverse [7] becoming available in conjunction with automated captioning methods like BLIP-2 [23], recent works [25, 33, 50, 60] trained on such datasets have showcased better performance and stronger generalizability. Despite this, more and more GPU resources are required for training such methods. These recent works [25, 33, 50] also predominantly choose point clouds as their 3D representation. The point clouds are typically limited in resolution and have a domain gap with real-world images, and thus these point cloud based methods can not effectively leverage the 2D priors from CLIP. Uni3D [60] proposed a training regime for incorporating 2D priors with point cloud as input. However, their model requires significant scaling (1B parameters) for the best performance. In this work, we instead choose multi-view images as our



(a) We use multi-view images, instead of point-clouds, to represent the shape.



(b) Accuracy on Objaverse-LVIS with all models trained on *Ensembled (no LVIS)*. Our Duoduo CLIP is fast to train, relatively small while also achieves the best performance.

Figure 1: We propose Duoduo CLIP, a simple model for 3D shape understanding that represents the shape with a multi-view images encoder instead of a point-cloud (PC) encoder. Compared to recent PC-based methods (e.g. OpenShape [25], Uni3D [60]), our model is both accurate and efficient.

shape representation. This not only allows for an easier extension and a more natural way to adapt off-the-shelf 2D representation models. Our Duoduo CLIP also results in more efficient training. As shown in Figure 1b, our model not only has much stronger generalization on shapes that were not seen during training with a modest model size, but also significantly lowers the amount of compute resources required for training (see Table 1). While some recent work [24, 39] also explore using multi-images with CLIP, their methods do not investigate the use of contrastive learning and only focus on zero/few-shot performance on small-scale datasets.

Using multi-view images also offers greater flexibility in many scenarios. Point cloud based methods require a fairly complete scan of the object, which can be challenging to obtain. In contrast, our model can encode objects from a variable number of frames (1 to M), with more frames capturing more details. Note that we use frames and views interchangeably. This makes our model plug-and-play for any method using image features for encoding 3D objects, enhancing performance with multiple frames. Additionally, previous methods that only train on synthetic objects have limited performance on real-world objects. We further train both our model point cloud based methods on real photos and densely reconstructed objects. Due to artifacts in the point cloud reconstruction pipeline, our model outperforms on real-world objects. Performance is boosted with additional multi-view images where point clouds aren’t available, demonstrating our model’s potential for scaling as more data becomes available.

In summary, our Duoduo CLIP model provides the following: **Simple model.** We average embeddings across views of an object to obtain 3D representations, while modifying the attention layers to span multiple frames of the shape to enable information flow across frames in the model. **Better efficiency.** We explore several strategies for efficiently fine-tuning off-the-shelf CLIP models, including training only the attention layers and selectively choosing the number of layers to train without hurting performance. **More flexible representation.** We showcase benefits of choosing multi-view images as a more flexible 3D representation over point clouds on real-world objects. Furthermore, we also demonstrate better text to shape retrieval with more fine-grained descriptions.

## 2 Related Work

There is a large literature of work on 3D representation learning from 3D data either using supervised training [31, 34] or using self-supervised learning (with reconstruction loss [5], contrastive learning [48], masked prediction [54], and others). Here we focus on work that learns aligned representation spaces between text and either 2D or 3D.

**2D-text joint representation.** Modeling multiple modalities through a shared representation has been explored through early works [10, 11, 21, 47] by aligning images and text embeddings. With the introduction of the InfoNCE loss [29], ConVIRT [57] proposed using contrastive learning with InfoNCE style loss to learn joint text and image embeddings. This was popularized by follow-up work such as CLIP [35] and ALIGN [20], which demonstrated that by scaling up training on a large-scale dataset, the learned embeddings can be useful for many downstream tasks such as classification, retrieval, grounding and generation. Followup work [20, 28, 51, 52, 55] has since been proposed to improve upon the formulation or training. There have also been attempts such as MERU [8] that use a hyperbolic embedding space to better model the hierarchical relations between text and images.

**3D-text joint representation.** Text2Shape [4] was one of the first works that introduced a captioned text and 3D dataset and used metric learning to learn an aligned space between text and 3D shapes. Follow-up work investigated how to improve the aligned representation for text-to-shape retrieval with triplet loss [41] and contrastive losses [36, 45, 49]. Prior work also investigated the use of CLIP to align the embeddings [36, 43, 49]. ULIP [49] used frozen CLIP text-image encoders, and trained only the point-cloud encoder. However, the generalizability of these works were limited by the available dataset size at the time. With the introduction of larger scale 3D datasets such as Objaverse [7], and the use of LVLMs for captioning 3D datasets [25, 27], more recent work [25, 50] were able to train with larger datasets of paired text and 3D shapes. OpenShape [25] and ULIP-2 [50] were among the first to use such datasets to train a point cloud encoder aligned with text using contrastive learning. TMM [58] leverages additional adapters to better align with the pre-trained CLIP models. Uni3D [60] exploits 2D priors within pre-trained large-scale vision models and maps point cloud patches to image patches within pre-trained ViTs to enable the scaling of even larger models. VIT-LENS [22] follows a similar pipeline by training a point cloud embedding layer and perceiver model to map to a frozen CLIP model. RECON++ [33] similar to RECON [32] employs both contrastive and MAE [15] reconstruction losses with an additional multi-view image matching cost. These recent works typically rely on frozen text and image encoders, and all used point-cloud encoders. Our work shows that taking embeddings of multi-view images is more efficient and works better with real-world images.

**Multi-view images for text-3D representations.** Multi-view images have long been used to represent 3D shapes [2, 13, 37, 40, 46], with recent work [24, 39] using multi-view images for shape representation by aggregating CLIP features. While these works also use CLIP with multi-view images, our focus is whether using a trainable multi-view shape encoder as a drop-in-replacement for the point-cloud encoder in contrastive settings such as OpenShape will result in better shape-representation for downstream tasks. These works do not focus on improved representation learning, but on how to use prompting to select better views or view aggregation and improve shape classification. There is also a line of work [17, 56, 61] that uses multi-view depth maps from point cloud to adapt CLIP models for 3D. However, the focus of these methods is still on point clouds and the models show limited performance on large-scale datasets [25, 50].

### 3 Method

Our Duoduo CLIP learns a shape representation by using contrastive learning to encode multi-view images into a pre-aligned text-image space. Our contrastive learning framework is similar to previous works [25, 49, 50, 58, 60], with a shape encoder  $E^S$  and frozen image  $E^I$  and text  $E^T$  encoders from a pre-trained CLIP model. The key difference of our model is that we replace the point cloud based shape encoder with one that uses multi-view images. Figure 1a shows a comparison of our model to prior work, and Figure 2 shows the details of our multi-view shape encoder.

To perform training, the dataset is organized into triplets of  $(S_i, I_i, T_i)$ , where  $S$  is the shape representation,  $I$  are rendered images of the 3D object and  $T$  is the corresponding text description. Embeddings are calculated for each modality  $f_i^S = E^S(S_i)$ ,  $f_i^I = E^I(I_i)$  and  $f_i^T = E^T(T_i)$ . The asymmetric contrastive loss [57] between any two modalities is:

$$l_i^{a \rightarrow b} = -\log \frac{\exp(\langle f_i^a, f_i^b \rangle) / \tau}{\sum_{k=1}^N \exp(\langle f_i^a, f_k^b \rangle) / \tau} \quad (1)$$

where  $a, b$  is any two modalities,  $\tau$  is the temperature and  $N$  is the batch size. Then, the full loss is:

$$L_{CON} = \frac{1}{4N} \sum_{i=1}^N (l_i^{S \rightarrow T} + l_i^{T \rightarrow S} + l_i^{S \rightarrow I} + l_i^{I \rightarrow S}) \quad (2)$$

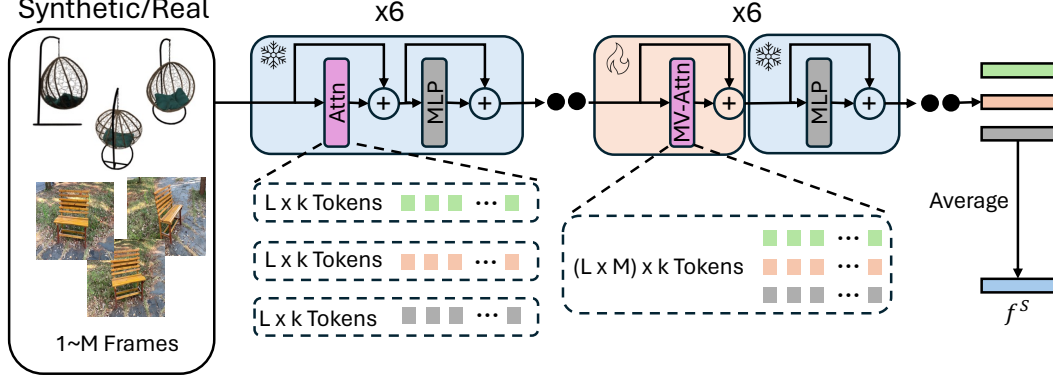


Figure 2: Our multi-view encoder takes a variable number  $[1, M]$  of images as input and outputs a single shape embedding. The first few layers of the ViT model are frozen (blue) and attention operates on the individual frames in parallel. For the latter layers, the attention layers are trainable (orange) and modified to attend over all  $M$  views. The embeddings for each frame are averaged to get the final embedding. Note that only major components of the model are depicted.

**Multi-view shape encoder.** For our multi-view shape encoder, we use rendered images of the object. Note that the input shape and image representations are the same, i.e.  $S_i = I_i = \{r_1, \dots, r_m\}$ , where  $r_j$  is a rendered frame, and  $m$  is the number of multi-views.  $E^I$  and  $E^S$  share the same network architecture, with the main difference between  $E^I$  and  $E^S$  is that  $E^I$  is frozen, while we train  $E^S$ . Weights for  $E^S$  are initialized from  $E^I$ . Empirically, we found it was useful to keep the contrastive losses  $l_i^{S \rightarrow I} + l_i^{I \rightarrow S}$ . We suspect that by keeping  $E^I$  frozen and the contrastive loss with the original image embeddings, our  $E^S$  can learn a good representation that is close to the text embeddings, but does not drift too much away from the initial image embeddings.

For both  $E^S$  and  $E^I$  we average the extracted embeddings for all  $m$  views to produce a single latent representation for an object:  $f_i^S = E^S(S_i) = \frac{1}{m} \sum_{j=1}^m \text{ViT}(S_i)[j]$ , where ViT [9] is the backbone encoder. Here we abuse the notation a bit, since our method allows interaction between views in the model, the index operation gets the corresponding embedding from the  $j$ -th frame's [CLS] token. We initialize  $E_S$  initially from  $E^I$ . During training, we randomly sample 1 to  $M$  views for each step so that the model is robust to a variable number of views.

**Multi-view attention.** We incorporate information flow between views by modifying the self-attention layers to attend over tokens across multiple views similar to recent multi-view aware methods like MVDream [38]. The original self-attention formulation [44] is  $\text{Attention}(Q, K, V) = \text{softmax}(\frac{QK^T}{\sqrt{d_k}} V)$ , where  $Q, K, V \in R^{L \times k}$ , and  $L$  is the token length for a single image after patchify operations and  $k$  is the channel dimension. For cross-view attention we aggregate token features across  $m$  multi-views such that  $Q^{\text{MV}}, K^{\text{MV}}, V^{\text{MV}} \in R^{(L \times m) \times k}$  (MV stands for multi-view) and the  $\text{Attention}(Q^{\text{MV}}, K^{\text{MV}}, V^{\text{MV}})$  can be calculated without changing the parameters of the original model. After attention, the views are separated and processed in parallel in other parts of the model. This mechanism helps the model reason between different views of the object and aggregate the most important information across all tokens.

**Trainable layers.** To reduce the memory needed for fine-tuning, we only train the self-attention layers. We further cut down on memory usage by reducing the number of trainable layers. Since the non-trainable self-attention layers have only been trained to see patches of a single image, we only enable the multi-view attention layers for the unfrozen attention layers (see Figure 2).

## 4 Experiments

To compare our Duoduo CLIP to prior work, we conduct experiments showing shape classification on a collection of 3D assets (on Objaverse-LVIS in Section 4.2), real-world multi-view images (on MVImgNet in Section 4.3), and more fine-grained text-to-shape retrieval (Section 4.4). We first describe the experimental setup including implementation details and the datasets we use.

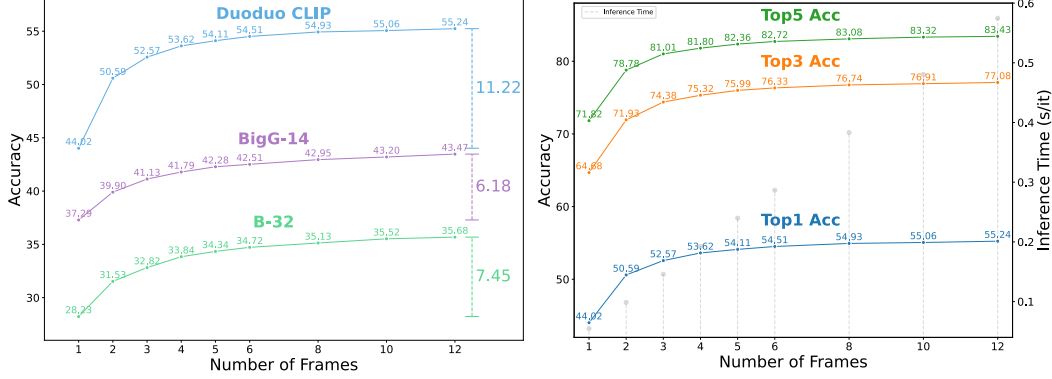


Figure 3: **Left.** We compare the Top 1 accuracies on Objaverse-LVIS for our model (Duoduo CLIP) and two pretrained CLIP models (zero shot) for different number of frames. B-32 is the model we initialize from and train with and BigG-14 is the model used by OpenShape. The dashed lines show the difference between using 1 and 12 frames. **Right.** We show the Top1, Top3 and Top5 accuracies for our model for 1 to 12 frames (note the y-axis starts at 40). Gray dashed lines shows the inference time(s) for 1 iteration and batch size 200 at different number of frames.

#### 4.1 Experimental setup

**Implementation details.** All of our models are trained with 16-bit mixed precision and a batch size of 1600 for 80 epochs. We use a learning rate of  $5e-5$  with cosine annealing. At each training step we randomly sample 1 to 6 multi-views for a batch of objects. The pretrained CLIP model used for initialization as well as the contrastive target is the ViT-B/32 CLIP model with checkpoint *laion2b\_s34b\_b79k* from the open source implementation OpenCLIP [18]. Additionally, we re-implemented OpenShape with 16-bit mixed precision training without projection layers for faster training in some baselines, indicated by OpenShape<sup>†</sup>.

**3D Datasets.** We follow OpenShape [25] and train our model on a combination of four datasets consisting of Objaverse [7], ABO [6], ShapeNet [3] and 3D-FUTURE [12]. Text for the shapes consists of captions produced by image-captioning models and filtered text descriptions from metadata of the 3D objects crawled from the web (see Liu et al. [25] for details). In total, the combined dataset contains  $\sim 874k$  shapes, with 46k shapes within the LVIS subset of Objaverse which are used for evaluation. As in OpenShape [25], we consider two variations of the data: 1) *Ensembled* which contains all shapes, and 2) *Ensembled (no LVIS)* which excludes shapes from the LVIS subset.

**Renderings.** We use images from Zero123 [26], which provides renderings of most shapes from Objaverse from 12 random views using spherical sampling. The shapes not included in Zero123 (a few remaining objects in Objaverse and the other 3 datasets) are rendered using their Blender<sup>1</sup> script to match the shapes in OpenShape. We render 12 views for all these objects.

**Real-world data.** MVImgNet [53] consists of multi-view images for 220k real-world objects over 238 categories. We first filter objects that has at least 12 multi-views to obtain  $\sim 190k$  remaining objects, where 12 views are evenly sampled. BLIP-2 [23] is then used to produce captions for each of the views. To compare with point cloud based methods, we use the MVPNet subset containing  $\sim 87k$  objects with densely reconstructed point clouds. After the preprocessing and filtering above, we obtain from MVPNet,  $\sim 66k$  objects for the train split and  $\sim 16k$  objects for the validation set, which has 180 categories. Note that the objects in the training and validation splits for MVPNet are disjoint but are both included in MVImgNet.

#### 4.2 Classification on Objaverse-LVIS

We conduct classification experiments on Objaverse-LVIS to investigate the performance of different variants of Duoduo CLIP and compare our model to prior work. As default settings for our experiments in this section, we use 12 multi-views to encode an object for evaluation. And only the

<sup>1</sup><https://www.blender.org/>

Table 2: Classification accuracy on Objaverse-LVIS trained on *Ensembled (no LVIS)* and *Ensembled*. The zero shot CLIP (B-32 and BigG-14) models are not trained on 3D data and serve as baselines. For each model, we indicate the representation used for computing the embeddings, multi-view (MV) or point-cloud (PC), and the shape encoder (Enc) architecture that is used. Our multi-view based Duoduo CLIP is able to outperform point-cloud based approaches with the exception of Uni3D is a large model with 1B parameters. † indicates our reimplementation of OpenShape which is faster and outperforms the original OpenShape.

Method	Rep	Enc	<i>Ensembled (no LVIS)</i>			<i>Ensembled</i>		
			Top1	Top3	Top5	Top1	Top3	Top5
ZS B-32 (12F)	MV	Avg	35.7	54.8	62.1	35.7	54.8	62.1
ZS BigG-14 (12F)	MV	Avg	43.5	64.2	71.3	43.5	64.2	71.3
ULIP [49]	PC	PointBERT	21.4	38.1	46.0	26.8	44.8	52.6
OpenShape [25]	PC	PointBERT	39.1	60.8	68.9	46.8	69.1	77.0
OpenShape†	PC	PointBERT	–	–	–	50.0	72.0	79.2
TAMM [58]	PC	PointBERT	42.0	63.6	71.7	50.7	73.2	80.6
Uni3D [60]	PC	3D VIT	47.2	68.8	76.1	<b>55.3</b>	76.7	82.9
ShapeLLM [33]	PC	RECON++	–	–	–	53.7	75.8	82.0
VIT-LENS [22]	PC	VIT-LENS <sub>G</sub>	50.1	71.3	78.1	52.0	73.3	79.9
Duoduo CLIP (5F)	MV	MVA	51.3	73.1	79.9	54.1	76.0	82.4
Duoduo CLIP (12F)	MV	MVA	<b>52.7</b>	<b>74.5</b>	<b>81.3</b>	55.2	<b>77.1</b>	<b>83.4</b>

multi-view attention of the latter 6 layers of the model is trained (total 12 layers). We run evaluations with 3 different seeds and average the results for experiments. Unless otherwise stated models are trained with the *Ensembled* dataset. For classification, we use do nearest neighbor search of the multi-view shape embedding with class embeddings. As in OpenShape, for each class label, we construct several sentences with the label and then take the average of the sentence embeddings as the class embedding. The final class chosen is the class with the highest average similarity between the class embedding and the shape embedding.

We compare the performance of our model against two CLIP models for different numbers of frames in Figure 3, and recent state-of-the-art models in Table 2. For the CLIP models, we selected VIT with B-32 (the model that our Duoduo CLIP is initialized with), and BigG-14 (the CLIP teacher model used by OpenShape). Both models are run in a zero-shot manner without training on additional 3D data (the weights are frozen, with embeddings from the image encoder averaged).

**How well does performance scale with number of views?** Having a more complete view of a 3D object is important for 3D representation learning as elements of the object may be occluded for certain views. Thus we investigate how the number of views affects the classification accuracy. From Figure 3 (left), we see that our model performance scales better as the amount of information (views) increases compared to the zero-shot CLIP models (11.22 for our Duoduo CLIP, and 7.45 for B-32, the model we used for initializing our weights). This suggests that our training strategy of randomly sampling 1 to 6 views during training is effective in letting the model learn to leverage the number of views given to it. Although, the accuracy increases as the number of multi-views increases, the inference time also increases (Figure 3 right). As the accuracy tapers off as we increase the number of views, to avoid additional computational cost during inference, we use 12 views as the default.

**How many multi-views to beat a point cloud?** Compared with using multi-views, using a point cloud representation offers good coverage of the entire geometry of the 3D object. Thus, we ask the question of how many views does it take to match existing methods on the Objaverse-LVIS classification task. We compare against ULIP [49], OpenShape [25], TAMM [58] that use point clouds with PointBERT [54] as the 3D encoder, but different ways of fine-tuning the 3D encoder. We also compare against more recent methods [22, 33, 60] that are the current top-performing methods on Objaverse-LVIS. From Table 2, on the *Ensembled* dataset, we are able to beat most previous methods with 5 multi-views except for Uni3D which has a much larger model (1B parameters). When we increase to 12 frames we are on par and even surpass Uni3D. This is also while using much fewer resources as seen in Table 1.

**Does multi-views generalize better compared to point cloud?** From the *Ensembled (no LVIS)* column of Table 2, we see that even the zero-shot BigG-14 model used as the teacher model for OpenShape beats it. Suggesting that the CLIP models already generalize well to unseen data, and point cloud methods potentially having worse generalization on unseen shapes. With our model that is further trained on *Ensembled (no LVIS)* we surpass point cloud methods by a large margin. Showing that fine-tuning the CLIP model better preserves their generalization ability.

Table 3: Multi-view attention (MVA) ablation of accuracy on Objaverse-LVIS.

Method	Frames	Top 1	Top 3	Top 5
-MVA	6	54.22	76.13	82.74
+MVA	6	54.59	76.46	82.89
-MVA	12	55.02	76.92	83.49
+MVA	12	55.32	77.08	83.49

Table 4: Number of layers ablation. Accuracy on Objaverse-LVIS.

Method	Top 1	Top 3	Top 5
3 layers	53.77	75.8	82.41
6 layers	55.24	77.08	83.43
12 layers (full)	55.32	77.08	83.49

**Does multi-view attention help?** We verify the effectiveness of our cross view attention in Table 3. For both -MVA and +MVA, we train all 12 attention layers, with the difference being +MVA has the cross-views attention enabled. We see that using multi-view attention helps the performance most in boosting Top1 accuracy for both 6-frame and 12-frame evaluations.

**Do we need to train all the layers?** We conduct an ablation to see if it is necessary to train all 12 layers. In Table 4, we show the accuracy for restricting the training to the last 3 and 6 MVA layers vs the full 12 MVA layers. We see that the number of trainable layers can be cut by half with minimal losses to accuracy, while further cuts start to hurt model performance. Training only half the layers reduces the VRAM usage by roughly half and allows us to train on GPUs with less memory. By restricting the training to the last 6 MVA layers, we can shift from training on 4×A40s (48 GB) to 4×A5000s (24 GB) (see Table 1).

Table 5: MVImgNet classification comparison.

Method	Top 1	Top 3	Top 5
ZeroShot B-32 (12F)	52.68	70.99	77.22
OpenShape†	3.55	8.94	12.70
OpenShape† (+MVPNet)	54.35	71.62	77.81
Ours (12F)	49.16	66.96	74.12
Ours (+MVPNet) (1F)	59.23	76.12	81.74
Ours (+MVPNet) (6F)	64.18	80.80	85.92
Ours (+MVPNet) (12F)	64.44	81.11	85.97
Ours (+MVImgNet) (1F)	61.75	79.07	84.18
Ours (+MVImgNet) (6F)	65.70	82.44	87.08
Ours (+MVImgNet) (12F)	<b>66.06</b>	<b>82.72</b>	<b>87.21</b>

Table 6: Text to shape retrieval comparison. Methods are trained on the Text2Shape [4] dataset (T2S) or *Ensembled*.

Model	Data	RR@1	RR@5
Text2Shape [4]	T2S	0.40	2.37
Y2Seq2Seq [14]	T2S	2.93	9.23
Parts2Words [41]	T2S	12.72	32.98
TriCoLo [36]	T2S	12.22	32.23
MXM-CLR [45]	T2S	16.83	39.06
ZeroShot B-32	Images	11.90	27.85
OpenShape†	Ens.	10.53	25.94
Uni3D-G	Ens.	10.78	26.37
Duoduo CLIP	Ens.	<b>15.90</b>	<b>34.08</b>

### 4.3 Classification on real-world data

To investigate how well our Duoduo CLIP works on real-world images, we evaluate on multi-view images from MVImageNet. For these experiments, we take our Duoduo CLIP model trained on the *Ensembled* dataset and add additional training data from MVImgNet. We consider two sets of data from MVImgNet, the MVPNet training split of objects or the entire MVImgNet (after our preprocessing and filter). For comparison with point cloud based methods, we evaluate on the validation set of MVPNet. As a representative of point cloud based methods, we choose OpenShape as it is relatively resource-light compared to other point cloud methods.

**Classification results.** We report accuracy results on MVPNet in Table 5. For OpenShape, the top-1 accuracy is extremely low (only 3.55% top-1) when evaluating on MVPNet directly with the model trained on *Ensembled* only. We suspect this is due to noisy reconstructed point clouds and inconsistent orientations compared to the training data. After training on MVPNet data, OpenShape’s performance



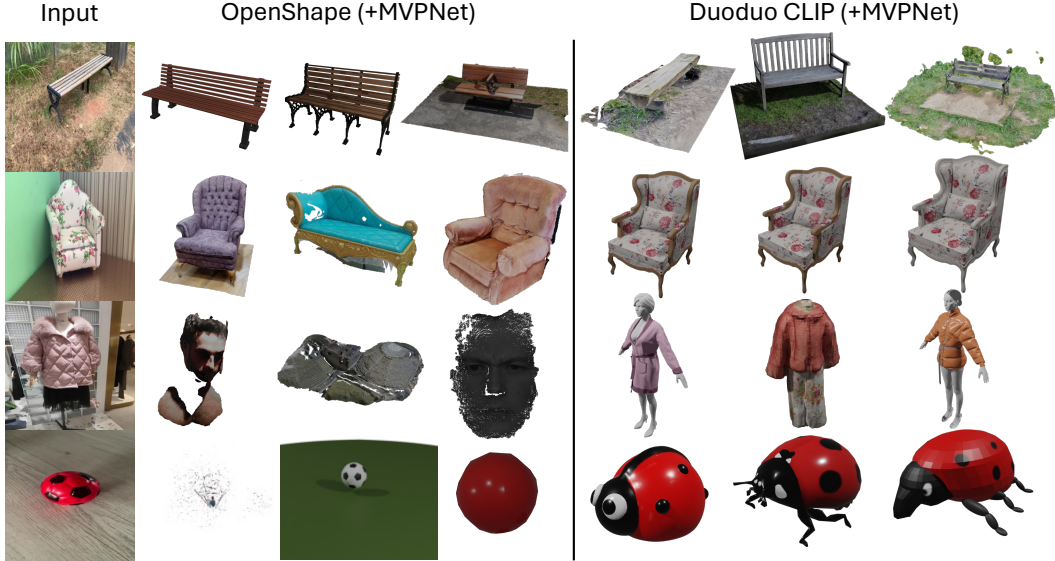


Figure 4: Retrieval results for OpenShape and Duoduo CLIP given input images from MVPNet. We perform retrieval with 12 input images, on the left most column we show one of the frames of the query object. For both methods we show the top 3 retrieval results using Objaverse as a retrieval library. Overall, Duoduo CLIP retrieves shapes that are more similar to the query image, while OpenShape sometimes retrieves broken geometry (row 3).

improves significantly. For our Duoduo CLIP, even without training on MVImgNet or MVPNet data, our model achieves a top-1 accuracy of 49.16%. However, this is lower than the zero-shot CLIP B-32 model that our model is initialized from, suggesting possible overfitting to synthetic data. When we include training with multi-view images from MVPNet, our method surpasses both OpenShape and the zero-shot CLIP B-32 model even when just using one 1 view. Performance is further boosted when trained on the entire MVImgNet, highlighting the advantages of our Duoduo CLIP which uses multi-view images over OpenShape’s point clouds. By using multi-view images, we have better generalization on unseen data due to the priors from initializing with CLIP B-32. We also can train on more data, as multi-view images are more readily available compared to point clouds.

**Retrieval examples.** In Figure 4, we present example retrieval results for querying Objaverse objects using images from the MVPNet validation set. We compare retrievals using OpenShape (+MVPNet) and Duoduo CLIP (+MVPNet). For OpenShape, we use 12 query images for each object, encode them with the frozen BigG-14 CLIP model, and average the image embeddings to obtain the query embedding.<sup>2</sup> This embedding is then matched against a database of point cloud embeddings of Objaverse objects to retrieve the top 3 results. For our method, Duoduo CLIP encodes both the query and Objaverse objects using 12 multi-view images.

From Figure 4, we see that for basic objects like benches, both methods are able to retrieve plausible objects. For the armchair (row 2), while OpenShape retrieved objects of the same semantic class, our Duoduo CLIP retrieved armchairs that has better matching textures. This is because multi-view images can represent textures better than point clouds. Note that some retrieved objects look similar due to duplicate objects in Objaverse. For the jacket (row 3), the objects returned by OpenShape have broken geometry and are incoherent. We hypothesize this may happen when the sampled points produce embeddings that are by chance similar to the query image. This issue is also present last example (a red and black soccer ball) where the first object retrieved by OpenShape has broken geometry. However, our method also fails in this case, as our model retrieves ladybugs with red wings and black dots that resemble the soccer ball. Interestingly, OpenShape is able to retrieve a soccer ball and a red ball. This can indicate that point cloud based methods may be more robust to geometric properties of the object compared to the rendered images. However, we find that overall the retrieved objects from our method is more consistent.

<sup>2</sup>For the largest BigG-14 CLIP model, OpenShape does not use any linear projection layer  $g^I$



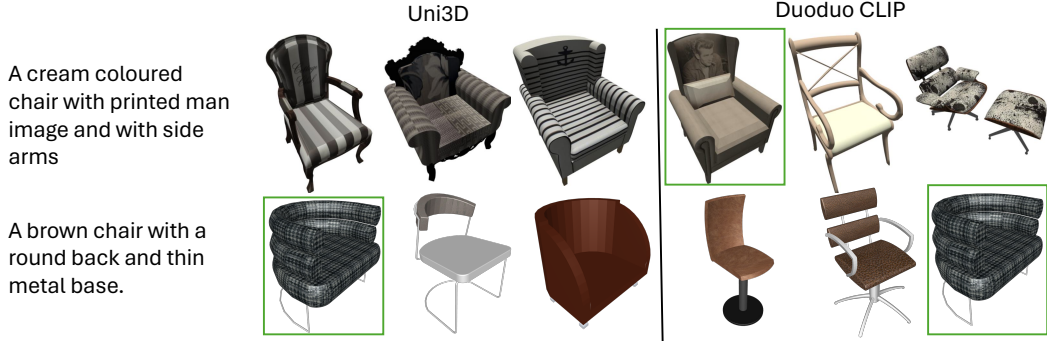


Figure 5: Retrieval using fine-grained text from the Text2Shape dataset. On the left is the input text description and we show the top 3 retrieval results for Uni3D and Duoduo CLIP with the ground truth shape highlighted in green.

#### 4.4 Fine grained text-to-shape retrieval

Previous evaluations focused on classification or image-based retrieval and do not assess how well the methods align fine-grained text descriptions with 3D models. To evaluate this aspect, we use the test split of Text2Shape [4], which contains  $\sim 1.4\text{k}$  tables and chairs from ShapeNet and  $\sim 7.4\text{k}$  human-captioned descriptions ( $\sim 5$  per shape). We report the shape retrieval rates at 1 and 5.

**Retrieval performance.** We compare the performance of our model to prior work in Table 6. We also include previous state-of-the-art methods that were trained on the Text2Shape dataset. Overall, compared to other methods trained on the *Ensembled* dataset, our method demonstrates superior performance. The zero-shot performance alone is impressive, surpassing point cloud methods. Notably, we observed a significant discrepancy between the zero-shot CLIP model reported by Ruan et al. [36] and our findings, where the LAION checkpoint trained by OpenCLIP significantly outperforms the original OpenAI checkpoint. Lastly, our model approaches the performance of the SOTA method trained directly on Text2Shape, indicating that there is still much to explore regarding more fine-grained text alignment in large-scale text-to-3D models.

**Retrieval examples.** We present example retrieval results compared to Uni3D in Figure 5. Generally, for text descriptions emphasizing complex textures, such as the ‘man image’ in the first row, our model successfully retrieves the corresponding ground truth 3D model. However, for descriptions focusing on geometric properties, like ‘round back’ in the second row, point cloud-based methods tend to retrieve shapes that better match the specified criteria.

## 5 Limitations and Future Work

We introduced Duoduo CLIP, an efficient joint text and 3D representation method that leverages multi-view images and surpasses current point cloud based state-of-the-art methods across almost all quantitative metrics while using significantly fewer resources on both synthetic and real datasets.

However, our method sometimes fails in cases requiring geometric understanding, as seen in the qualitative retrieval results from images or text. This is an inherent advantage of point clouds, as each point contains three-dimensional coordinates. To address this, we could explore additional inputs to the model such as depth or normal images of the objects, which provide more geometric information, especially with recent depth estimation methods becoming better. Another potential way to improve performance is with LLMs, as demonstrated by Tang et al. [42], where representations from ULIP-2 were used by an LLM to boost performance and enable question-answering applications. Using our model might further increase performance, offering the flexibility of requiring only a single or a sparse number of images as input. Banani et al. [1] also point out the relative weakness of CLIP pretraining on both 3D structure and consistency benchmarks compared to newer SSL methods [30, 59], which can potentially replace the current pretraining framework used by most works.

Overall, we believe that our method will provide better resource scaling compared to point cloud based methods as more 3D data becomes available in the future.

**Acknowledgements.** This work was funded by a CIFAR AI Chair, a NSERC Discovery grant, and a CFI/BCKDF JELF grant.

## References

- [1] Mohamed El Banani, Amit Raj, Kevis-Kokitsi Maninis, Abhishek Kar, Yuanzhen Li, Michael Rubinstein, Deqing Sun, Leonidas Guibas, Justin Johnson, and Varun Jampani. Probing the 3D awareness of visual foundation models. In *Proc. of the Conference on Computer Vision and Pattern Recognition (CVPR)*, 2024. URL <https://doi.org/10.48550/arXiv.2404.08636>.
- [2] Gary Bradski and Stephen Grossberg. Recognition of 3-D objects from multiple 2-D views by a self-organizing neural architecture. In *From Statistics to Neural Networks: Theory and Pattern Recognition Applications*, pages 349–375. Springer, 1994.
- [3] Angel X Chang, Thomas Funkhouser, Leonidas Guibas, Pat Hanrahan, Qixing Huang, Zimo Li, Silvio Savarese, Manolis Savva, Shuran Song, Hao Su, et al. ShapeNet: An information-rich 3D model repository. *arXiv preprint arXiv:1512.03012*, 2015. URL <https://doi.org/10.48550/arXiv.1512.03012>.
- [4] Kevin Chen, Christopher B Choy, Manolis Savva, Angel X Chang, Thomas Funkhouser, and Silvio Savarese. Text2shape: Generating shapes from natural language by learning joint embeddings. In *Proceedings of the Asian Conference on Computer Vision (ACCV)*, pages 100–116. Springer, 2019. URL <https://doi.org/10.48550/arXiv.1803.08495>.
- [5] Zhiqin Chen and Hao Zhang. Learning implicit fields for generative shape modeling. In *Proc. of the Conference on Computer Vision and Pattern Recognition (CVPR)*, pages 5939–5948, 2019. URL <https://doi.org/10.48550/arXiv.1812.02822>.
- [6] Jasmine Collins, Shubham Goel, Kenan Deng, Achleshwar Luthra, Leon Xu, Erhan Gundogdu, Xi Zhang, Tomas F Yago Vicente, Thomas Dideriksen, Himanshu Arora, et al. ABO: Dataset and benchmarks for real-world 3D object understanding. In *Proc. of the Conference on Computer Vision and Pattern Recognition (CVPR)*, pages 21126–21136, 2022. URL <https://doi.org/10.48550/arXiv.2110.06199>.
- [7] Matt Deitke, Dustin Schwenk, Jordi Salvador, Luca Weihs, Oscar Michel, Eli VanderBilt, Ludwig Schmidt, Kiana Ehsani, Aniruddha Kembhavi, and Ali Farhadi. Objaverse: A universe of annotated 3D objects. In *Proc. of the Conference on Computer Vision and Pattern Recognition (CVPR)*, 2023. URL <https://doi.org/10.48550/arXiv.2212.08051>.
- [8] Karan Desai, Maximilian Nickel, Tanmay Rajpurohit, Justin Johnson, and Shanmukha Ramakrishna Vedantam. Hyperbolic image-text representations. In *Proc. of the International Conference on Machine Learning (ICML)*, pages 7694–7731. PMLR, 2023. URL <https://doi.org/10.48550/arXiv.2304.09172>.
- [9] Alexey Dosovitskiy, Lucas Beyer, Alexander Kolesnikov, Dirk Weissenborn, Xiaohua Zhai, Thomas Unterthiner, Mostafa Dehghani, Matthias Minderer, Georg Heigold, Sylvain Gelly, Jakob Uszkoreit, and Neil Houlsby. An image is worth 16x16 words: Transformers for image recognition at scale. In *Proc. of the International Conference on Learning Representations (ICLR)*, 2021. URL <https://doi.org/10.48550/arXiv.2010.11929>.
- [10] Fartash Faghri, David J Fleet, Jamie Ryan Kiros, and Sanja Fidler. VSE++: Improving visual-semantic embeddings with hard negatives. In *Proc. of the British Machine Vision Conference (BMVC)*, 2018. URL <https://doi.org/10.48550/arXiv.1707.05612>.
- [11] Andrea Frome, Greg S Corrado, Jon Shlens, Samy Bengio, Jeff Dean, Marc’Aurelio Ranzato, and Tomas Mikolov. Devise: A deep visual-semantic embedding model. *Advances in neural information processing systems*, 26, 2013. URL [https://papers.nips.cc/paper\\_files/paper/2013/file/7cce53cf9057744271720a370c3c723-Paper.pdf](https://papers.nips.cc/paper_files/paper/2013/file/7cce53cf9057744271720a370c3c723-Paper.pdf).
- [12] Huan Fu, Rongfei Jia, Lin Gao, Mingming Gong, Binqiang Zhao, Steve Maybank, and Dacheng Tao. 3D-FUTURE: 3D furniture shape with texture. *International Journal of Computer Vision (IJCV)*, 129: 3313–3337, 2021. URL <https://doi.org/10.48550/arXiv.2009.09633>.
- [13] Abdullah Hamdi, Silvio Giancola, and Bernard Ghanem. MVTN: Multi-view transformation network for 3D shape recognition. In *Proc. of the International Conference on Computer Vision (ICCV)*, 2021. URL <https://doi.org/10.48550/arXiv.2011.13244>.
- [14] Zhizhong Han, Mingyang Shang, Xiyang Wang, Yu-Shen Liu, and Matthias Zwicker. Y2Seq2Seq: Cross-modal representation learning for 3D shape and text by joint reconstruction and prediction of view and word sequences. In *AAAI Conference on Artificial Intelligence*, volume 33, pages 126–133, 2019. URL <https://doi.org/10.48550/arXiv.1811.02745>.
- [15] Kaiming He, Xinlei Chen, Saining Xie, Yanghao Li, Piotr Dollár, and Ross Girshick. Masked autoencoders are scalable vision learners. In *Proc. of the Conference on Computer Vision and Pattern Recognition (CVPR)*, pages 16000–16009, 2022. URL <https://doi.org/10.48550/arXiv.2111.06377>.
- [16] Chenguang Huang, Oier Mees, Andy Zeng, and Wolfram Burgard. Visual language maps for robot navigation. In *International Conference on Robotics and Automation (ICRA)*, pages 10608–10615. IEEE, 2023. URL <https://doi.org/10.48550/arXiv.2210.05714>.
- [17] Tianyu Huang, Bowen Dong, Yunhan Yang, Xiaoshui Huang, Rynson WH Lau, Wanli Ouyang, and Wangmeng Zuo. CLIP2Point: Transfer CLIP to point cloud classification with image-depth pre-training.

- In *Proc. of the International Conference on Computer Vision (ICCV)*, pages 22157–22167, 2023. URL <https://doi.org/10.48550/arXiv.2210.01055>.
- [18] Gabriel Ilharco, Mitchell Wortsman, Ross Wightman, Cade Gordon, Nicholas Carlini, Rohan Taori, Achal Dave, Vaishaal Shankar, Hongseok Namkoong, John Miller, Hannaneh Hajishirzi, Ali Farhadi, and Ludwig Schmidt. OpenCLIP, July 2021. URL <https://doi.org/10.5281/zenodo.5143773>.
  - [19] Krishna Murthy Jatavallabhula, Alihusein Kuwajerwala, Qiao Gu, Mohd Omama, Tao Chen, Alaa Maalouf, Shuang Li, Ganesh Iyer, Soroush Saryazdi, Nikhil Keetha, Ayush Tewari, Joshua B. Tenenbaum, Celso Miguel de Melo, Madhava Krishna, Liam Paull, Florian Shkurti, and Antonio Torralba. ConceptFusion: Open-set multimodal 3D mapping. In *Robotics: Science and Systems (RSS)*, 2023. URL <https://doi.org/10.48550/arXiv.2302.07241>.
  - [20] Chao Jia, Yinfei Yang, Ye Xia, Yi-Ting Chen, Zarana Parekh, Hieu Pham, Quoc Le, Yun-Hsuan Sung, Zhen Li, and Tom Duerig. Scaling up visual and vision-language representation learning with noisy text supervision. In *Proc. of the International Conference on Machine Learning (ICML)*, pages 4904–4916. PMLR, 2021. URL <https://doi.org/10.48550/arXiv.2102.05918>.
  - [21] Ryan Kiros, Ruslan Salakhutdinov, and Richard S Zemel. Unifying visual-semantic embeddings with multimodal neural language models. *arXiv preprint arXiv:1411.2539*, 2014. URL <https://doi.org/10.48550/arXiv.1411.2539>.
  - [22] Weixian Lei, Yixiao Ge, Jianfeng Zhang, Dylan Sun, Kun Yi, Ying Shan, and Mike Zheng Shou. VIT-lens: Towards omni-modal representations. In *Proc. of the Conference on Computer Vision and Pattern Recognition (CVPR)*, 2024. URL <https://doi.org/10.48550/arXiv.2311.16081>.
  - [23] Junnan Li, Dongxu Li, Silvio Savarese, and Steven Hoi. BLIP-2: Bootstrapping language-image pre-training with frozen image encoders and large language models. In *Proc. of the International Conference on Machine Learning (ICML)*, pages 19730–19742. PMLR, 2023. URL <https://doi.org/10.48550/arXiv.2301.12597>.
  - [24] Dongyun Lin, Yi Cheng, Shangbo Mao, Aiyuan Guo, and Yiqun Li. PEVA-net: Prompt-enhanced view aggregation network for zero/few-shot multi-view 3D shape recognition. *arXiv preprint arXiv:2404.19168*, 2024. URL <https://doi.org/10.48550/arXiv.2404.19168>.
  - [25] Minghua Liu, Ruoxi Shi, Kaiming Kuang, Yin hao Zhu, Xuanlin Li, Shizhong Han, Hong Cai, Fatih Porikli, and Hao Su. OpenShape: Scaling up 3D shape representation towards open-world understanding. In A. Oh, T. Neumann, A. Globerson, K. Saenko, M. Hardt, and S. Levine, editors, *Advances in Neural Information Processing Systems*, volume 36, pages 44860–44879. Curran Associates, Inc., 2023. URL [https://proceedings.neurips.cc/paper\\_files/paper/2023/file/8c7304e77c832ddc70075dfee081ca6c-Paper-Conference.pdf](https://proceedings.neurips.cc/paper_files/paper/2023/file/8c7304e77c832ddc70075dfee081ca6c-Paper-Conference.pdf).
  - [26] Ruoshi Liu, Rundi Wu, Basile Van Hoorick, Pavel Tokmakov, Sergey Zakharov, and Carl Vondrick. Zero-1-to-3: Zero-shot one image to 3D object. In *Proc. of the International Conference on Computer Vision (ICCV)*, pages 9298–9309, 2023. URL <https://doi.org/10.48550/arXiv.2303.11328>.
  - [27] Tiange Luo, Chris Rockwell, Honglak Lee, and Justin Johnson. Scalable 3D captioning with pretrained models. *Advances in Neural Information Processing Systems*, 36, 2024. URL <https://doi.org/10.48550/arXiv.2306.07279>.
  - [28] Norman Mu, Alexander Kirillov, David Wagner, and Saining Xie. SLIP: Self-supervision meets language-image pre-training. In *Proc. of the European Conference on Computer Vision (ECCV)*, pages 529–544. Springer, 2022. URL <https://doi.org/10.48550/arXiv.2112.12750>.
  - [29] Aaron van den Oord, Yazhe Li, and Oriol Vinyals. Representation learning with contrastive predictive coding. *arXiv preprint arXiv:1807.03748*, 2018. URL <https://doi.org/10.48550/arXiv.1807.03748>.
  - [30] Maxime Oquab, Timothée Darcet, Théo Moutakanni, Huy Vo, Marc Szafraniec, Vasil Khalidov, Pierre Fernandez, Daniel Haziza, Francisco Massa, Alaaeldin El-Nouby, et al. DINOv2: Learning robust visual features without supervision. *Transactions on Machine Learning Research (TMLR)*, 2023. URL <https://doi.org/10.48550/arXiv.2304.07193>.
  - [31] Charles R Qi, Hao Su, Kaichun Mo, and Leonidas J Guibas. PointNet: Deep learning on point sets for 3D classification and segmentation. In *Proc. of the Conference on Computer Vision and Pattern Recognition (CVPR)*, pages 652–660, 2017. URL <https://doi.org/10.48550/arXiv.1612.00593>.
  - [32] Zekun Qi, Runpei Dong, Guofan Fan, Zheng Ge, Xiangyu Zhang, Kaisheng Ma, and Li Yi. Contrast with reconstruct: Contrastive 3D representation learning guided by generative pretraining. In *Proc. of the International Conference on Machine Learning (ICML)*, pages 28223–28243. PMLR, 2023. URL <https://doi.org/10.48550/arXiv.2302.02318>.
  - [33] Zekun Qi, Runpei Dong, Shaochen Zhang, Haoran Geng, Chunrui Han, Zheng Ge, Li Yi, and Kaisheng Ma. ShapeLLM: Universal 3D object understanding for embodied interaction. *arXiv preprint arXiv:2402.17766*, 2024. URL <https://doi.org/10.48550/arXiv.2402.17766>.
  - [34] Guocheng Qian, Yuchen Li, Houwen Peng, Jinjie Mai, Hasan Hammoud, Mohamed Elhoseiny, and Bernard Ghanem. PointNeXt: Revisiting PointNet++ with improved training and scaling strategies. *Advances in Neural Information Processing Systems*, 35:23192–23204, 2022. URL <https://doi.org/10.48550/arXiv.2206.04670>.
  - [35] Alec Radford, Jong Wook Kim, Chris Hallacy, Aditya Ramesh, Gabriel Goh, Sandhini Agarwal, Girish Sastry, Amanda Askell, Pamela Mishkin, Jack Clark, et al. Learning transferable visual models from

- natural language supervision. In *Proc. of the International Conference on Machine Learning (ICML)*, pages 8748–8763. PMLR, 2021. URL <https://doi.org/10.48550/arXiv.2103.00020>.
- [36] Yue Ruan, Han-Hung Lee, Yiming Zhang, Ke Zhang, and Angel X Chang. TriCoLo: Trimodal contrastive loss for text to shape retrieval. In *Proceedings of the IEEE/CVF Winter Conference on Applications of Computer Vision (WACV)*, pages 5815–5825, 2024. URL <https://doi.org/10.48550/arXiv.2201.07366>.
- [37] Yu-Te Shen, Ding-Yun Chen, Xiao-Pei Tian, and Ming Ouhyoung. 3D model search engine based on lightfield descriptors. In *Eurographics (Posters)*, 2003.
- [38] Yichun Shi, Peng Wang, Jianglong Ye, Mai Long, Kejie Li, and Xiao Yang. MVDream: Multi-view diffusion for 3D generation. In *Proc. of the International Conference on Learning Representations (ICLR)*, 2023. URL <https://doi.org/10.48550/arXiv.2308.16512>.
- [39] Dan Song, Xinwei Fu, Weizhi Nie, Wenhui Li, and Anan Liu. MV-CLIP: Multi-view CLIP for zero-shot 3D shape recognition. *arXiv preprint arXiv:2311.18402*, 2023. URL <https://doi.org/10.48550/arXiv.2311.18402>.
- [40] Hang Su, Subhansu Maji, Evangelos Kalogerakis, and Erik Learned-Miller. Multi-view convolutional neural networks for 3D shape recognition. In *Proc. of the International Conference on Computer Vision (ICCV)*, pages 945–953, 2015. URL <https://doi.org/10.48550/arXiv.1505.00880>.
- [41] Chuan Tang, Xi Yang, Bojian Wu, Zhizhong Han, and Yi Chang. Parts2words: Learning joint embedding of point clouds and texts by bidirectional matching between parts and words. In *Proc. of the Conference on Computer Vision and Pattern Recognition (CVPR)*, pages 6884–6893, 2023. URL <https://doi.org/10.48550/arXiv.2107.01872>.
- [42] Yuan Tang, Xu Han, Xianzhi Li, Qiao Yu, Yixue Hao, Long Hu, and Min Chen. MiniGPT-3D: Efficiently aligning 3D point clouds with large language models using 2D priors. *arXiv preprint arXiv:2405.01413*, 2024. URL <https://doi.org/10.48550/arXiv.2405.01413>.
- [43] Jesse Thomason, Mohit Shridhar, Yonatan Bisk, Chris Paxton, and Luke Zettlemoyer. Language grounding with 3D objects. In *Conference on Robot Learning*, pages 1691–1701. PMLR, 2022. URL <https://doi.org/10.48550/arXiv.2107.12514>.
- [44] Ashish Vaswani, Noam Shazeer, Niki Parmar, Jakob Uszkoreit, Llion Jones, Aidan N Gomez, Łukasz Kaiser, and Illia Polosukhin. Attention is all you need. *Advances in neural information processing systems*, 30, 2017. URL <https://doi.org/10.48550/arXiv.1706.03762>.
- [45] Ye Wang, Bowei Jiang, Changqing Zou, and Rui Ma. MXM-CLR: A unified framework for contrastive learning of multifold cross-modal representations. *arXiv preprint arXiv:2303.10839*, 2023. URL <https://doi.org/10.48550/arXiv.2303.10839>.
- [46] Xin Wei, Ruixuan Yu, and Jian Sun. View-GCN: View-based graph convolutional network for 3D shape analysis. In *Proc. of the Conference on Computer Vision and Pattern Recognition (CVPR)*, pages 1850–1859, 2020. URL <https://doi.org/10.1109/CVPR42600.2020.00192>.
- [47] Jason Weston, Samy Bengio, and Nicolas Usunier. WSABIE: Scaling up to large vocabulary image annotation. In *International Joint Conference on Artificial Intelligence*, 2011.
- [48] Saining Xie, Jiatao Gu, Demi Guo, Charles R Qi, Leonidas Guibas, and Or Litany. PointContrast: Unsupervised pre-training for 3D point cloud understanding. In *Proc. of the European Conference on Computer Vision (ECCV)*, pages 574–591. Springer, 2020. URL <https://doi.org/10.48550/arXiv.2007.10985>.
- [49] Le Xue, Mingfei Gao, Chen Xing, Roberto Martín-Martín, Jiajun Wu, Caiming Xiong, Ran Xu, Juan Carlos Niebles, and Silvio Savarese. ULIP: Learning a unified representation of language, images, and point clouds for 3D understanding. In *Proc. of the Conference on Computer Vision and Pattern Recognition (CVPR)*, pages 1179–1189, 2023. URL <https://doi.org/10.48550/arXiv.2212.05171>.
- [50] Le Xue, Ning Yu, Shu Zhang, Junnan Li, Roberto Martín-Martín, Jiajun Wu, Caiming Xiong, Ran Xu, Juan Carlos Niebles, and Silvio Savarese. ULIP-2: Towards scalable multimodal pre-training for 3D understanding. In *Proc. of the Conference on Computer Vision and Pattern Recognition (CVPR)*, 2024. URL <https://doi.org/10.48550/arXiv.2305.08275>.
- [51] Jianwei Yang, Chunyuan Li, Pengchuan Zhang, Bin Xiao, Ce Liu, Lu Yuan, and Jianfeng Gao. Unified contrastive learning in image-text-label space. In *Proc. of the Conference on Computer Vision and Pattern Recognition (CVPR)*, pages 19163–19173, 2022. URL <https://doi.org/10.48550/arXiv.2204.03610>.
- [52] Jiahui Yu, Zirui Wang, Vijay Vasudevan, Legg Yeung, Mojtaba Seyedhosseini, and Yonghui Wu. CoCa: Contrastive captioners are image-text foundation models. *Transactions on Machine Learning Research (TMLR)*, 2022. URL <https://doi.org/10.48550/arXiv.2205.01917>.
- [53] Xianggang Yu, Mutian Xu, Yidan Zhang, Haolin Liu, Chongjie Ye, Yushuang Wu, Zizheng Yan, Chenming Zhu, Zhangyang Xiong, Tianyou Liang, et al. MVImgNet: A large-scale dataset of multi-view images. In *Proc. of the Conference on Computer Vision and Pattern Recognition (CVPR)*, pages 9150–9161, 2023. URL <https://doi.org/10.48550/arXiv.2303.06042>.
- [54] Xumin Yu, Lulu Tang, Yongming Rao, Tiejun Huang, Jie Zhou, and Jiwen Lu. Point-BERT: Pre-training 3D point cloud transformers with masked point modeling. In *Proc. of the Conference on Computer Vision and Pattern Recognition (CVPR)*, pages 19313–19322, 2022. URL <https://doi.org/10.48550/arXiv.2111.14819>.

- [55] Xiaohua Zhai, Xiao Wang, Basil Mustafa, Andreas Steiner, Daniel Keysers, Alexander Kolesnikov, and Lucas Beyer. LIT: Zero-shot transfer with locked-image text tuning. In *Proc. of the Conference on Computer Vision and Pattern Recognition (CVPR)*, pages 18123–18133, 2022. URL <https://doi.org/10.48550/arXiv.2111.07991>.
- [56] Renrui Zhang, Ziyu Guo, Wei Zhang, Kunchang Li, Xupeng Miao, Bin Cui, Yu Qiao, Peng Gao, and Hongsheng Li. PointCLIP: Point cloud understanding by CLIP. In *Proc. of the Conference on Computer Vision and Pattern Recognition (CVPR)*, pages 8552–8562, 2022. URL <https://doi.org/10.48550/arXiv.2112.02413>.
- [57] Yuhao Zhang, Hang Jiang, Yasuhide Miura, Christopher D Manning, and Curtis P Langlotz. Contrastive learning of medical visual representations from paired images and text. In *Machine Learning for Healthcare Conference*, pages 2–25. PMLR, 2022. URL <https://doi.org/10.48550/arXiv.2010.00747>.
- [58] Zhihao Zhang, Shengcao Cao, and Yu-Xiong Wang. TAMM: Triadapter multi-modal learning for 3D shape understanding. In *arXiv preprint arXiv:2402.18490*, 2024. URL <https://doi.org/10.48550/arXiv.2402.18490>.
- [59] Jinghao Zhou, Chen Wei, Huiyu Wang, Wei Shen, Cihang Xie, Alan Yuille, and Tao Kong. iBOT: Image BERT pre-training with online tokenizer. In *Proc. of the International Conference on Learning Representations (ICLR)*, 2022. URL <https://doi.org/10.48550/arXiv.2111.07832>.
- [60] Junsheng Zhou, Jinsheng Wang, Baorui Ma, Yu-Shen Liu, Tiejun Huang, and Xinlong Wang. Uni3D: Exploring unified 3D representation at scale. In *Proc. of the International Conference on Learning Representations (ICLR)*, 2024. URL <https://doi.org/10.48550/arXiv.2310.06773>.
- [61] Xiangyang Zhu, Renrui Zhang, Bowei He, Ziyu Guo, Ziyao Zeng, Zipeng Qin, Shanghang Zhang, and Peng Gao. PointCLIP v2: Prompting CLIP and GPT for powerful 3D open-world learning. In *Proc. of the International Conference on Computer Vision (ICCV)*, pages 2639–2650, 2023. URL <https://doi.org/10.48550/arXiv.2211.11682>.